ISSN: 2319-8753

International Journal of Innovative Research in Science, Engineering and Technology

(An ISO 3297: 2007 Certified Organization)

Vol. 3, Issue 6, June 2014

Properties of Spin Bath of Graphene–Like Nanocarbon

Arvind Kumar [1], Prashant S. Alegaonkar [2,*]

Department of Applied Physics, Defence Institute of Advanced Technology, Girinagar, Pune 411 025, MS, India

ABSTRACT: Understanding and controlling the complex environment of solid–state quantum–bits is a central challenge in quantum information science and spintronics. We report on behavior of electron spin bath embedded in graphene–like nanocarbon (GNCs) superlattice. The GNCs were few layered, mixed sp^2–sp^3 phase, and contained local heavy vacancy disorder. The electron spectroscopy for chemical analysis indicated that, ratio of sp^2:sp^3 was 2:3 with native oxygen of ~ 6.75 atomic% attached to the sp^3 sites. The spin transport data was obtained using electron spin resonance spectroscopy, carried out at 123–473K. Transport parameters were derived by deconvoluting Dysonian linewidth, and estimating anisotropy in Lande's g–factor. The parameters such as spin–spin, spin–lattice relaxation time, and spin–orbit coupling constant were estimated and analyzed for their temperature and interdependence. The analysis revealed that, feeble magnetization exist due to charge inhomogeneities in GNCs yielding weak delocalization of π–electrons. However, this delocalization is sufficiently useful to provide desired spin degrees of freedom to the spin bath. Analysis showed that, the bath have, practically, no effect of 2p–oxygen orbital quenching, the O–impurity existed in GNCs. These results open the door to understand coherent spin transport in GNCs. Designing spin bath with tuneable spin degrees of freedom is essential for solid state quantum–bits; vital organ of future quantum computational device. Details are presented.

KEYWORDS: quantum–bits; coherent spin bath; spin–orbit coupling; spin–lattice relaxation; Dysonian lineshape (key words)

I. INTRODUCTION

The paramagnetic resonances arising from the conduction electron in carbon could be harnessed for processing information, in the form of strings of quantum–bits (qubits) [1]. These electrons diffuse in and out of the surface of the carbon and would have decisive effect on transport of information for storage, and secured communication [2]. The conduction electrons are assumed to mobile like free particles and collective electron magnetic moments is treated as the bath of free particle carrying quantized spin moments. In general, such quantum systems *communicate* with their environment via up or down orientations of spin [3]. The spin degrees of freedom of electron bath endowed to its lattice is on the *talking term* and could be exploited, primarily, using spin–orbit–(SO)–interactions [4]. However, crucial requirements on such spin bath are quantum entanglement [5], spin–phonons coupling [6], weak decoherence [7], and hyperfine interaction with surrounding nuclear spin [8]. In carbon, especially, graphene, the SO interaction has intrinsic [9], Bychkov–Rashba [10], ripple [4], and extrinsic contributions [11]. These interactions are supposed to be weak, in μeV regime [12], due to low atomic number of carbon. However, interest of the whole analysis will lie not in the diffusion effect itself but in quantifying properties of such spin bath.

The purpose of the present communication is to address behavior of such spin bath embedded in graphene–like nanocarbon (GNCs) superlattice. The electron spectroscopy for chemical analysis indicated that, composition of sp^2:sp^3 was 2:3 and GNCs contained oxygen, mainly, attached to the sp^3 moieties. The spin transport data was obtained over 123–473K, using electron spin resonance spectroscopic technique, at X–band. Analysis revealed that, feeble magnetization exists due to puddeling effect which lead to weak delocalization of π–electrons. Practically, no effect of oxygen 2p–orbital quenching had been observed due to O–impurity that existed in GNCs. Nonetheless, the π–electrons delocalization is sufficient to offer desired spin degrees of freedom to the spin bath of GNCs. Understanding spin transport in GNCs may provide clue to design spin bath with tuneable spin degrees of freedom; essential for solid state quantum–bits, essential for future quantum computational device.

ISSN: 2319-8753

International Journal of Innovative Research in Science, Engineering and Technology

(An ISO 3297: 2007 Certified Organization)

Vol. 3, Issue 6, June 2014

II. EXPERMINTAL

In the present work, Graphene–like nanocarbon sheets (GNCs) were synthesized according to protocol reported in ref [13]. To comment, briefly, the material obtained by our synthesis methodology was graphene–like nanosheets and not graphene. The material contains mixed, sp^2 + sp^3 phase rather than pure sp^2 bonded graphene network. This system is typically 2–5 layers and each layer contains heavy local disorder.

The elemental composition, purity and bond chemical environment of GNCs was analyzed using electron spectroscopy chemical analysis (ESCA) technique. ESCA measurements were conducted with Omicron ESCA Probe (Omicron Nanotechnology) system. Standard conditions required a vacuum better than 2×10^9 mbar, with a monochromatic aluminium K_α source and source power of 200 W (10 kV × 20 mA). The spot size was ~1 mm in cross scans, with pass energy of 100 eV for wide scans with step size 0.100eV. For all samples, spectra for barium, nitrogen, oxygen, and carbon have been acquired, respectively, in a period of 7, 5, 2 min and 55 sec, keeping other parameters invariant. Number of scans has been varied for element to element from 3 to 10.

The ESR measurements were carried out using a standard ESR set up equipped with electromagnet, microwave bridge, resonant cavity, waveguide circuitry and spectrometer consol. The measurements were performed at microwave frequency of ~ 9.1 GHz. (X–band). The maximum microwave output was varied from sample to sample in the range 985 µW to 1000 µW. The quality factor of the resonating cavity was 12000. The modulation frequency was kept constant at 100 kHz by adjusting the band pass filter parameter of the lock–in–amplifier. The static magnetic field was swept slowly at a spectrum–point time constant 0.1 sec over the range 300 mT to 370 mT with the amplitude of modulation frequency kept at 6 kHz. The field centre was 336 mT and ESR line width, $\Delta H = 0.05$ mT. The signal–to–noise ratio was computed to be 20 at 300K with 1s per spectrum–point constant. The sensitivity of the system was 7.0×10^9 spins / 0.1 mT and resolution 2.35 µT. The measurements were carried out at a temperature range 123–473K. And the first derivative of the paramagnetic absorption signal was recorded for GNCs.

III. RESULTS AND DISCUSSION

For the analysis of ESCA spectrum, in terms of contribution from individual components representing various species, each obtained peak was fitted by a combination of components by minimizing the total squared–error (least squared–error) of the fit. Individual components were represented by a convolution of a Lorentzian function representing the life time broadening and a Gaussian function to account for the instrumental resolution [18]. The Gaussian broadening was kept same for different components. A Shirley background–function is considered to account for the inelastic background in the ESCA spectrum. Fig. 1 shows recorded ESCA peak of C–1s recorded for GNCs. The C–1s core spectrum of GNCs appeared at binding energy of 285.33 eV. The full width at half maximum (FWHM) of C–1s is 2.50 eV. The peak intensity is 3.35×10^5 Counts per second for GNCs.

The elemental analysis carried out for revealed that atomic % (at %) of carbon estimated in GNCs samples is ~ 93.00 %. Further, the C–1s peak is deconvoluted into three chemical components. The C_1 peak located at 289.20 eV is attributed to O=C–OH i.e for sp^2 carbon. The composition of O=C–OH moiety within Carbon envelop is 9.32 at%. The C_2 at 286.23 eV is assigned to sp^3 based –C–O–C– group. And C_3 appeared at 285.07 eV corresponds to C–C of sp^3 origin. The compositions of C_2 and C_3 are 40.45 and 43.23 at%, respectively. These two peaks are the characteristic peaks for GNCs phase. The overall range of peak intensity of C–1s peak, recorded for GNCs, indicates that, p–type dopant also exist due to physically adsorbed oxygen moiety. The p–type dopant is available in GNCs in the form of bound Dirac hole. In general, the GNCs contain native oxygen ~ 6.75 at%. Thus ESCA analysis indicates that, GNCs contain ~ 93 at% carbon and ~ 6.75 at% oxygen in the form of O=C–OH (carboxyl) and –C–O–C (epoxy–like) sites. The exchange interaction could be dominant at oxygen site that exchange couple hole, at oxygen site. Further, exchange coupling could be dominant at sp^2/sp^3 interface too, due to availability of dangling electron bound to π–state. The ESCA analysis showed that, the population of sp^3 content is relatively high than sp^2.

ISSN: 2319-8753

International Journal of Innovative Research in Science, Engineering and Technology

(An ISO 3297: 2007 Certified Organization)

Vol. 3, Issue 6, June 2014

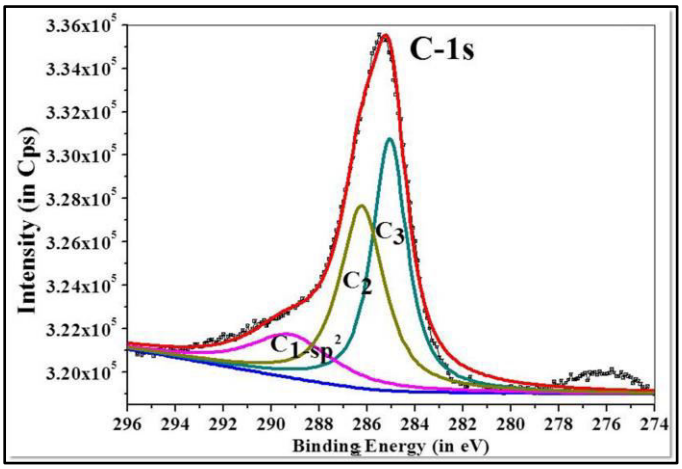

Fig. 1 Recorded C–1s ESCA spectrum for GNCs.

Fig. 2 shows ESR dispersion derivatives (*dy/dH*) as a function of magnetic field for GNCs. The inset shows Dysonian ratio (A/B) computed for ΔH_{pp} over the measured temperature range. The ΔH_{pp} has an azimuth angular dependence (θ) i.e. orientation of applied field with respect to the orientation of carbon planes of the samples. Since, measurements were conducted on the bulk powder specimen then: $\Delta H_{pp}(\theta) = sin^2(\theta)H_{\parallel} + cos^2(\theta)H_{\perp}$. Thus, the measured ΔH_{pp} consists of contribution from $H_{\parallel}$ as well as $H_{\perp}$ field components. The obtained and estimated values of transport parameters are almost constant over the measured temperature range. Hence, in subsequent discussions, temperature averaged magnitude of measured and estimated physical quantities are quoted (with standard deviation) using the symbol $<\ldots>_T$. The value of $<\Delta H_{pp}>_T$ is 0.5693 ± 0.03275 mT, for GNCs.

To describe, width of ESR lines, there are two common shapes: Gaussian and Lorentzian. The spectra are found to be asymmetric for GNCs and mixed Lorentzian–Gaussian. The magnitude of obtained $<\Delta H_{pp}>_T$ indicates that, there are more than two components of spin–lattice relaxation time (T_{sl}) involved into one overall line. The strength of T_{sl} is different and reflected in asymmetric lineshape. The asymmetry arises due to charge inhomogeneities, so called puddles, due to weak delocalization of π–states from bound π–electrons [15]. The charge inhomogeneities over the volume of the sample exceeds the natural line–width, $(1/\gamma T_{sl})$, where γ is gyromagnetic ratio. These puddles prevent relaxing electron from reaching the Dirac point, and they have the average minimal charge density as 10^9 cm^{-2}. The spins associated with these charge inhomogeneities, in various parts of the sample, find themselves in different field strength, and the resonance is narrowed in an inhomogeneous manner. The variations in A/B with temperature indicate that, the conductivity of samples varies with temperature [16].

ISSN: 2319-8753

International Journal of Innovative Research in Science, Engineering and Technology

(An ISO 3297: 2007 Certified Organization)

Vol. 3, Issue 6, June 2014

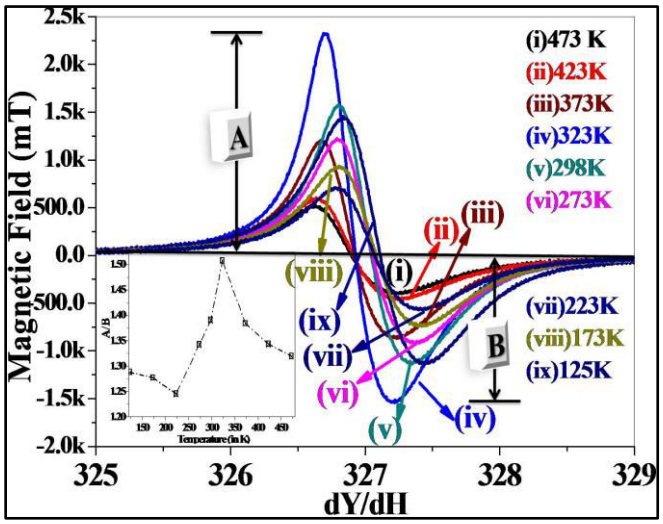

Fig. 2 ESR dispersion derivatives (dY/dH) as a function magnetic field for GNCs over the measured temperature range (i)–(ix) 473–125K. The spectra show unsymmetrical Dysonian absorption derivative line–shape on low field side. The arrows show magnitude of A and B. The inset shows variations in Dysonian lineshape ratio as a function of temperature.

TABLE I

Temperature (in K)	Δg
123	0.00457
173	0.00458
223	0.00459
273	0.00449
298	0.00453
323	0.00447
373	0.00452
423	0.00464
473	0.00449
$<A>_T$	$0.00453 \pm 4.73 \times 10^{-5}$

Table 1. Estimated Δg for GNCs. The Δg is difference between g–factor for non–degenerated Pauli gas to effective g–factor obtained for the samples, at the resonance field. The last row **$<A>_T$** indicates the temperature averaged value of Δg.

Another prominent component is the magnitude of g–factor, at which the resonance has occurred under applied microwave frequency. The g–factor characterizes the magnetic moment, and gyro–magnetic ratio associated with unpaired electrons in the material. If the angular momentum of a system is solely due to spin angular momentum, the tensor g–factor should be isotropic, with the value 2.00232. Any deviation from this value involves contributions of: (i) orbital moment from the excited state, and (ii) spin–spin interaction. However, the orbital moments interacts strongly with the crystalline fields and becomes decoupled from the spin, a process called *quenching*. The more incomplete the *quenching*, the farther the g–factor from the free electron value and results into the effective g–factor. The magnitude of effective g–factor is estimated for the GNCs. The effective g–factor is observed to be less than 2.00232. The difference Δg for the system is computed. The value of $<\Delta g>_T$ is found to be $0.00453 \pm 4.73 \times 10^{-5}$, for GNCs.

ISSN: 2319-8753

International Journal of Innovative Research in Science, Engineering and Technology

(An ISO 3297: 2007 Certified Organization)

Vol. 3, Issue 6, June 2014

For GNCs, there are ~ 6–7 oxygen atoms per 100 carbon atoms. Even though the isoelectronic carbon contains 6–7 at % oxygen the anisotropy in g–factor is too small. One can see that, values of Δg is unchanged upto third decimal place i.e. ≈ 0.004. The variations have been observed from the third decimal place onwards. Thus data indicate slightly anisotropic magnitudes of g–factors of the measured GNCs system. Thus, the spin originating from oxygen impurity has weak contribution to the spin bath of carbon inherited spin species [17]. The values also indicate that, the local magnetic environment in carbon system is distinctly different than that exist in a conventional magnetic material. Moreover, it gives a clue that the species responsible for the intense line is carbon. Thus contribution of orbital moments, and spin–spin interactions from oxygen species could be neglected and overall strength of this component seems to be less in GNCs. To evaluate contribution of each component we have analyzed spin–spin and spin–orbit interactions as discussed below:

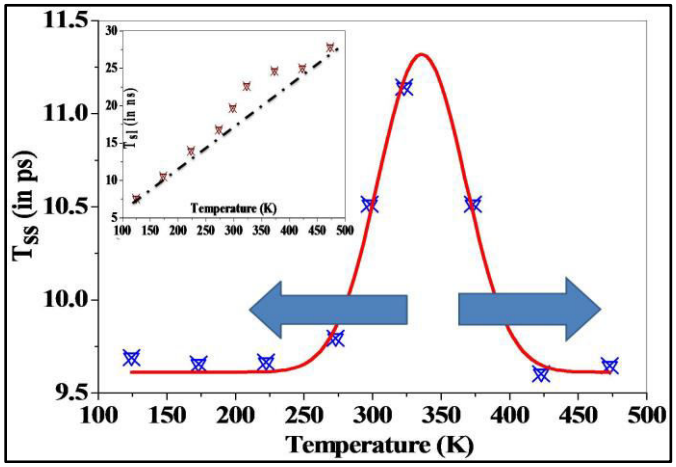

Fig. 3 Variations in spin–spin relaxation time (T_{ss}) as a function of temperature for GNCs. Arrows indicate, change in T_{ss} as temperature of spin bath moves away from room temperature window of ~ 75 K. Inset shows change in spin–lattice relaxation time (T_{sl}) with temperature.

To estimate them, magnitude of ΔH_{pp} bares important information about spin dynamics of the system, specifically T_{ss} which corresponds to electron spin–spin relaxation time. Due to external perturbation, the deformed spin system regains the state of equilibrium 'up' or 'down' over the characteristic time scale and is termed as spin–spin relaxation time. The entity ΔH_{pp} and T_{ss} are correlated by equation: $\Delta H_{pp} = 1/\gamma_e T_{ss}$, where, γ_e has magnitude 1.760859 X 10^{11} / sec–T, for electrons. The variations in T_{ss}, as a function of temperature, for GNCs is shown in Fig. 3. The magnitude of T_{ss}, at temperature window of ~ 300–375 K, is found to be greater than 11.01 ± 0.60 ps. As one move away from this window T_{ss} decreases by one order of magnitude. It is interesting to note that, T_{ss} varies ~ e^{-T^2}, where T is temperature.

TABLE II

Temperature (in K)	L_i (in meV)
123	18.68
173	18.96
223	18.80
273	18.19
298	18.59
323	18.07
373	18.10
423	18.07
473	18.55
$<A>_T$	18.49±0.32

Table 2: Variation in spin–orbit coupling constant (L_i) over measured temperature range.

ISSN: 2319-8753

International Journal of Innovative Research in Science, Engineering and Technology

(An ISO 3297: 2007 Certified Organization)

Vol. 3, Issue 6, June 2014

The principal parameter governing spintronic usability is spin–lattice relaxation time (T_{sl}) which quantifies variation of non–thermal spin state around the lattice. For spintronic applications, theoretical estimate of T_{sl} for graphene is 10–100 ns [14], whereas, experimental spin–transport measurements showed that it is as short as 60–150 psec [15]. The magnitude of T_{sl} is computed using relation: $\frac{1}{T_{sl}} = \frac{28.0\ GHz}{T\ (in\ K)} \times \Delta H_{pp}$. The variation in T_{sl} as a function of temperature for the measured carbon systems is shown in inset of Figure 3. For GNCs magnitude of $<T_{sl}>$ is 18.75 ± 6.99 ns. However, one can see that, over the measured temperature range T_{sl} varies by five fold i.e. from ~ 5 to 25 ns and change is almost linear. Basically, electron spin relax by transferring energy selectively to those lattice modes with which they resonate. The resonant modes are on *talking term* with the spins. And one can modify their *cross talk* by introducing break in the symmetry inversion (i.e.disorder) or adatom in the sp^2 carbon network. However, over the temperature, the resonant levels seems to be somewhat broadened for GNCs. In principle, the orbital and the spin angular moment have been considered separately; it is important to know the extent to which these are coupled. As a first approximation the two may be considered independently later introducing a small correction to account for the so called spin–orbit (SO) interaction. The pure, radical free, carbon system have, essentially, zero orbital angular momentum; the SO interaction is usually very small for such systems hence for most purposes attention may be focused wholly upon the spin angular momentum. However, SO interaction must necessarily be included in a discussion of the ESR behaviour, as presented below.

SO interaction is one of the most prominent modes of spin relaxation [18]. There are three principal sources of SO coupling, in graphene: intrinsic, Bychkov–Rashba (BR, related to structural symmetry break) and ripples (related to inevitable wrinkles/folding edges). However, it is not possible to estimate contribution of each component experimentally. Theoretical estimate for intrinsic SO coupling ranges 1 μeV–0.2 meV and BR 10–36 μeV/V/nm. Until recently, it has been reported that, curved carbon surfaces could have zero–spin splitting with SO coupling upto 3.4 meV [19]. The quantification of SO interaction could be done using correlation: $\Delta g = \alpha\left(\frac{Li}{\Delta}\right)$, where α, is band structure dependent constant ≈ 1, and L_i is spin–orbit coupling constant (SOCC). From the estimated value of Δg (in Table 1) and obtaining the magnitude of π–σ bandwidth, Δ, one can estimate L_i. A correlation of ΔH_{pp}, and optical bandwidth (Δ) has already been noted [19]. The values of Δ for GNCs is measured to be 3.380 eV. The existent knowledge about the SO interaction in carbon systems is not yet complete [20]. From the perspectives spintronic applications it is important to understand the role of electronic spin in sp^2+sp^3 network bonded environment of disordered GNCs. The value of $<L_i>_T$ 18.49 ± 0.32 meV, for GNCs. The ESCA analysis showed that, at% of native oxygen is ~ 6.75%. However, the orbital angular momentum contribution seems to be fully quenched from the spin bath of GNCs. The magnitude of L_i is found to be three orders of magnitude larger than reported, previously [20]. The GNCs are disordered, heterostructure sp^2+sp^3 network, in contrast to ordered sp^2 graphene carbon. The observed variations could also possibly be attributed to different spin and orbital angular momentum contribution of carbon in ordered and disordered sp^2 honeycomb network leading to entirely different type of exchange interactions [4]. Thus, analysis of spin–spin (T_{ss}), and spin–orbit (L_i) together with spin–lattice interactions (T_{sl}) indicates that spin degrees of freedom seems to be somewhat enhanced in GNCs. For realistic applications, spin bath with tuneable spin degrees of freedom is advantageous to manipulate, flip, and toggle the spin density wave. Thus, the SO interaction that couples electronic states with opposite spin projections in different bands, typically identified as spin–up and spin–down [20] seems to be stronger in GNCs.

IV. CONCLUSION

Thus, coherent spin bath is essentially important for setting up solid state qubit in any material. In conclusions, spin bath parameters were analyzed, for GNCs, over 125–475 K, using X–band ESR technique. The analysis was focused on deconvoluting Dysonian linewidth (ΔH_{pp}), and estimating anisotropy in Lande's g–factor (Δg). The linewidths were found to be asymmetric and mixed Lorentzian–Gaussian. The asymmetry was due to charge puddles leading to weak delocalization of π–states from bound π–electrons. The magnitude of $<\Delta H_{pp}>_T$ was found to be 0.5693 ± 0.03275 mT and indicative of more than two components of T_{sl} involved into one overall line. The change in A/B indicated that, the conductivity of GNCs varied with temperature. For GNCs, there were ~ 6–7 oxygen atoms per 100 carbon atoms. Even though the isoelectronic carbon contained ~ 6.75 at % oxygen, the anisotropy in g–factor is too small and <Δg>T was found to be $0.00453 \pm 4.73 \times 10^{-5}$. This indicated that, the orbital contribution of O–impurity was negligible compared to SO interactions of carbon inherent species. The magnitude of T_{ss}, varied ~ e^{-T^2} (T, temperature

ISSN: 2319-8753

International Journal of Innovative Research in Science, Engineering and Technology

(An ISO 3297: 2007 Certified Organization)

Vol. 3, Issue 6, June 2014

in K). At the temperature window of 300–375 K, T_{ss} was found to be 11.01 ± 0.60 ps and as one move away from this window T_{ss} decreased by one order of magnitude. For GNCs magnitude of $<T_{sl}>$ was found to be 18.75 ± 6.99 ns and over the temperature range T_{sl} varied by five fold i.e. from ~ 5 to 25 ns. The change in T_{sl} was almost linear. The SO interaction that couples electronic states with opposite spin projections in different bands, typically identified as spin–up and spin–down was found to be 18.49 ± 0.32 meV and seems to be stronger by three orders of magnitude in GNCs than graphene. Thus, analysis of spin–spin, and spin–orbit coupling together with spin–lattice interactions indicated that spin degrees of freedom seems to be somewhat enhanced in GNCs. For realistic applications, spin bath with tuneable spin degrees of freedom is advantageous to manipulate, flip, and toggle the spin density wave without a decoherence.

ACKNOWLEDGMENT

Authors are thankful to Defence Research and Development Organization (DRDO), Ministry of Defence, Government of India, for their financial assistance via DRDO–DIAT program on nano–materials funded by ER&IPR, DRDO. Authors are thankful to Dr Prahlada, The Vice Chancellor, DIAT, Pune. We would like to acknowledge SAIF, IIT Bombay, India for providing ESR measurements on commercial basis and Dr. K. R. Patil, National Chemical Lab., Pune for providing ESCA measurements.

REFERENCES

[1] P. Neumann, R. Kolesov, B. Naydenov, J. Beck, F. Rempp, M. Steiner, V. Jacques, G. Balasubramanian, M. L. Markham, D. J. Twitchen, S. Pezzagna, J. Meijer, J. Twamley, F. Jelezko, J. Wrachtrup, "Quantum register based on coupled electron spins in a room-temperature solid," Nature Physics, vol. 6, pp. 249–253, 28 February 2010.

[2] Z. Merali, "Quantum computing: The power of discord," Nature, Vol. 474, pp. 24–26, 1 June 2011.

[3] S.G. Carter, T. M. Sweeney, M. Kim, C. S. Kim, D. Solenov, S. E. Ecomomou, T. L. Reinecke, L. Yang, A. S. Bracker, and D. Gammon, "Quantum control of a spin quibit to a coupled to photonic crystal cavity," Nature Photonics, vol.7, pp. 329–334, 17 March 2013.

[4] D. H. Hernando, F. Guinea, A. Brataas, "Spin-orbit coupling in curved graphene, fullerenes, nanotubes, and nanotube caps," Phys. Rev. B, vol. 74, pp. 155426, 24 October 2006.

[5] T. Monz, P. Schindler, J. T. Barreiro, M. Chwalla, D. Nigg, W. A. Coish, M. Harlander, W. Hänsel, M. Hennrich, and R. Blatt, "14-Qubit Entanglement: Creation and Coherence," Phys. Rev. Lett., vol. 106, pp. 130506, 31 March 2011

[6] V.N. Golovach, A. V. Khaetskii, and D. Loss, "Phonon-Induced Decay of the Electron Spin in Quantum Dots," Phys. Rev. Lett., vol. 93, pp. 016601, 28 June 2004.

[7] L.Childress, M.V.G. Dutt, J. M.Taylor, A.S. Zibrov, F. Jrlezko, J. Wrachtrup, P. R. Hemmer, and M. D. Lukin, "Coherent Dynamics of Coupled Electron and Nuclear Spin Qubits in Diamond," Science, vol. 314, 281–285, 13 October 2006.

[8] O. V. Yazyev, "Hyperfine Interactions in Graphene and Related Carbon Nanostructures, " Nano Letters, vol. 8, pp. 1011–1015, 6 March 2008.

[9] C.L. Kane, and E.J. Mele, "Quantum Spin Hall Effect in Graphene," Phys. Rev. Lett., vol. 95, pp. 226801, 23 November 2005.

[10] Y.A. Bychkov, and E.I. Rashba, "Oscillatory effects and the magnetic susceptibility of carriers in inversion layers," J. Phys. C, vol. 17, pp. 6039, 30 November 1984.

[11] B. Dóra, F. Murány and F. Simon, "Electron spin dynamics and electron spin resonance in graphene," Europhysics Letter, Vol 92, pp. 17002, 22 October 2010.

[12] M. Gimitra, S. Konschuh, C. Ertler C. A. Draxl, and J. Fabian, "Band-structure topologies of graphene: Spin-orbit coupling effects from first principles," Phys. Rev. B, vol. 80, pp. 315431, 28 December 2009.

[13] A. Kumar, S. Patil, A. Joshi, V. Bhoraskar, S. Datar, and P. Alegaonkar, "Mixed phase, sp2–sp3 bonded, and disordered few layer graphene-like nanocarbon: Synthesis and characterizations," Appl. Surf. Sci., vol. 271, pp. 86–92, 8 February 2013.

[14] M. Sepioni, R. R. Nair, S. Rablen, J. Narayanan, F. Tuna, R. Winpenny, A. K. Geim, and I. V. Grigorieva1, "Limits on Intrinsic Magnetism in Graphene," Phys. Rev. Lett., vol. 105, pp. 207205, 12 November 2010.

[15] S. Talapatra, P. G. Ganesan, T. Kim, R. Vajtai, M. Huang, M. Shima, G. Ramanath, D. Srivastava, S. C. Deevi, and P. M. Ajayan, "Irradiation-Induced Magnetism in Carbon Nanostructures," Phys. Rev. Lett., vol. 95, pp. 097201, 23 August 2005

[16] G. Wagoner, "Spin Resonance of Charge Carrier in Graphite" Phys. Rev., vol. 118, pp. 647, 25 May 1960.

[17] S. Hino, K. Umishita, K. Iwasaki, K. Tanaka, T. Sato, T. Yamabe, K. Yoshizawa, and K.Okahara, "Electronic Structure of TDAE–C60 Complex," J. Phys. Chem. A, vol. 101, pp 4346–4350, 12 June 1997.

[18] C. Malitesla, "New Findings in Polypyrrole Chemical Structure by XPS Coupled to Chemical Derivatization Labelling." J. Elect. Spect. and Reltd. Phenomena, vol. 76, pp. 629-634, 29 December 1995.

[19] D. Khveshchenko, " Magnetic–Field–Induced Insulating Behavior in Highly Oriented Pyrolitic Graphite," Phys. Rev. Lett., vol. 87, pp. 206401, 24 October 2001.

[20] P. O. Lehtinen, A. S. Foster, A. Ayuela, A. Krasheninnikov, K. Nordlund, and R. M. Nieminen, "Magnetic Properties and Diffusion of Adatoms on a Graphene Sheet," Phys. Rev. Lett., vol. 91,pp. 017202, 30 June 2003.